Cracking, Fracture Assessment, and Repairs of Green River Bridge, I-26

John W. Fisher and Eric J. Kaufmann, *Lehigh University*
Michael J. Koob, *Wiss, Janney, Elstner Associates, Inc.*
Gerald White, *North Carolina Department of Transportation*

The Green River Bridge, I-26 near Asheville, North Carolina, was opened to traffic in 1969. In October 1992, during an inspection, two long transverse cracks were discovered in the bottom flange plate of a main girder; these cracks resulted in closure of the eastbound bridge. Numerous shorter cracks were observed at the web to flange plate connecting fillet welds throughout the girders. The Green River Bridge is a five-span, twin structure having a total length of 320 m (1,050 ft). Each bridge is a two-girder system, and ASTM A441 modified Corten B weathering steel was used to fabricate the bridge. The investigation into the cause of the cracking included metallographic and fractographic examination of core samples containing cracks, chemical composition and toughness testing of material, and instrumentation and field testing to determine live load stress levels. Test results of the flange plate material containing the large cracks showed it to have high carbon content, large grain structure, very low toughness, and high hardness. A field hardness survey was carried out on all bottom flange plates to determine locations of plates in the structure with similar properties. The fatigue and fracture assessment found that the cracks discovered in the Green River Bridge occurred at the time of fabrication. All cracks appeared to result from hydrogen-related cold cracking. Orientation of the large cracks was influenced by welding residual stresses that caused the crack tip to turn to a nearly horizontal orientation (parallel to the stress field). Because of this favorable crack tip orientation, the large cracks could tolerate dead and live load stresses and fatigue crack growth and brittle fracture were prevented. The main retrofit recommendation was to bolt cover plates on all bottom flange plates subjected to tensile stresses using high-strength bolts. This retrofit will provide internal redundancy in all spans and reduce live load stress range levels in the two-girder system by about 50 percent. Repairs were completed in October 1994.

The Green River Bridge, located about 50 km (30 mi) southeast of Asheville, North Carolina, carries Interstate 26 across the Green River. This twin structure consists of five spans having a total length of 320 m (1,050 ft): a continuous unit of spans 80, 100, and 80 m (260, 330, and 260 ft) long over the river and simple spans of 30.5 m (100 ft) at each end. A view looking west between the twin bridge structures is shown in Figure 1. Each bridge carries two lanes of traffic.

The steel superstructure consists of a two-girder system using welded girders 4.3 m (14 ft) deep spaced 7.3 m (24 ft) apart. Transverse floor beams frame into these girders on approximately 73-m (24-ft) centers and support two longitudinal deck stringers. A typical cross sec-

FIGURE 1 View looking west between twin bridge structures.

tion through the bridge is shown in Figure 2. The bridge is 25 years old, and ASTM A441 modified U.S. Steel Corten B weathering steel was used to fabricate the superstructure.

In October 1992, during a North Carolina Department of Transportation (NCDOT) inspection by an engineering consultant, two long transverse cracks were found in the bottom flange plate of a main girder 7.3 m (14 ft) deep. These cracks measured 100 and 70 mm (4 and 2¾ in.), respectively, and extended through the web-to-flange plate fillet weld with extension into the bottom flange plate (Figure 3). Further inspection found many shorter cracks, of lengths up to 19 mm (¾ in.) at the web-to-flange plate connecting fillet welds throughout the girders. Two typical cracks with lengths of approximately 19 mm (¾ in.) are shown in Figure 4.

After it discovered the two long cracks, NCDOT closed the eastbound bridge. The cracks were evaluated to determine their causes and to develop retrofit recommendations to repair the bridge structures. The evaluation included metallographic and fractographic studies on core samples removed from the eastbound bridge that contained cracks, instrumentation and field testing of the westbound bridge to measure live load stress levels, testing of flange plate hardness, removal of additional cores for material testing, and recommendations for retrofitting.

The information collected from the various tasks—particularly the testing, examination of core samples, and main retrofit recommendation—is reviewed. Using the repair recommendations for the steel superstructure from this study, NCDOT developed contract plans for repairing the bridge. In September 1994, the repairs were completed to both east- and westbound structures, and they were reopened to traffic.

Primary Girder Geometry

In general, the 4.3-m-deep welded plate girders are fabricated using flange plate 610 mm (24 in.) wide with varying thickness and a web plate 16 mm (⅝ in.) thick. The 30.5-m (100-ft) end spans use three bottom flange plates 610 mm (24 in.) wide by 25 mm (1 in.) thick. A total of 25 plates make up the bottom flange of each three-span continuous girder. These plates vary in thickness from 32 to 95 mm (1¼ to 3¾ in.) thick and 610 to 760 mm (24 to 30 in.). Bolted or welded splices are used between adjacent plates. Figure 5 shows a partial evaluation of the bridge girder with flange plate dimensions and splices indicated. In total, there are 124 bottom flange plates in the four primary girders of the two bridge structures.

Cracks and Sample Removal

Cracks in the web-to-bottom flange connecting weld were observed in both eastbound and westbound structures. However, cracks of significant size that extended into the girder flanges were found only in the eastbound structure. The greatest incidence of cracking was in Girder 301G1-3, where four cracks extended into the flange plate. Figure 5 shows the location of the large cracks found in Girder 301G1-3. To determine the causes of these cracks, cores were extracted that included the largest web-flange weld cracks in Girder 301G1-3, so that fractographic studies could be carried out, and these large cracks could be removed from the eastbound structure. Three cores 75 mm (3 in.) in diameter were removed with a hole saw and contained cracks originating from the web-flange fillet weld connection. A 25-mm (1-in.) hole was also removed with a hole saw at the parapet crack tip. These cores were designated as 17, 17-1, 23, and 25, as shown schematically in a plan view of the bottom flange in Figure 6. Core 17 contained the largest crack, which consisted of two transverse weld metal cracks on opposite sides of the web that extended into the flange plate. Core 17-1 was removed at the termination of the large crack about 100 mm (4 in.) from the web plate; it contains the crack tip. Figure 7 is a view of Core 17 showing the crack. Figure 8 shows a polished and etched cross section cut longitudinally through one fillet weld in Core 17. It also shows the transverse weld metal crack and crack extension into the flange plate. The curved orientation of the crack, becoming nearly parallel to the plate surface, is shown clearly and indicates that the cracks developed without significant load on the girder allowing the crack to follow the principal stresses from fabrication.

Core 23 and 25 also contained weld metal cracks in the web-flange plate fillet weld. The two cracks ob-

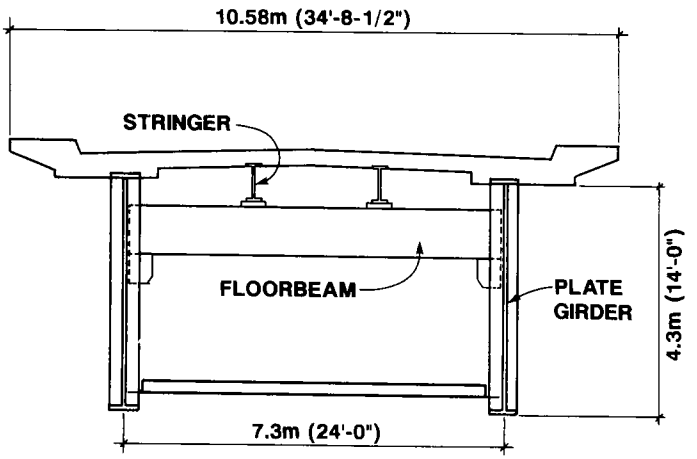

FIGURE 2 Typical cross section.

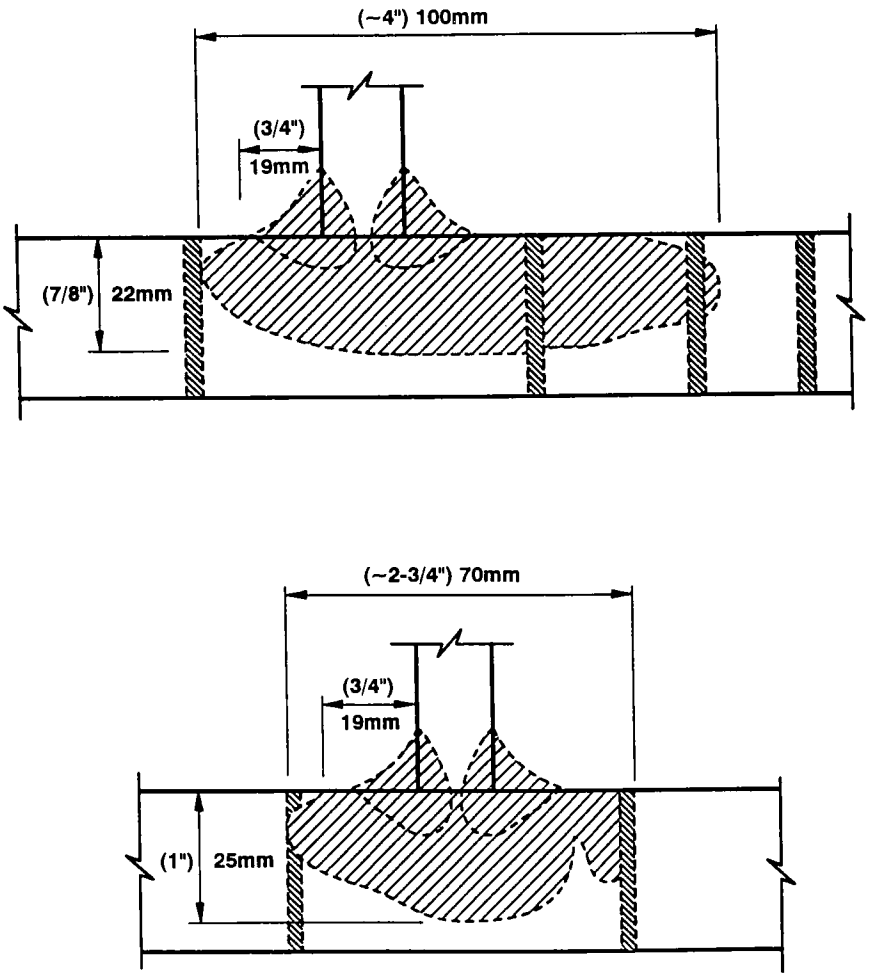

FIGURE 3 Projected crack geometry on plane perpendicular to girder flange: *top*, schematic of crack in flange at Core 17; *bottom*, schematic of crack in flange at Core 25.

FIGURE 4 Typical cracking found in web-to-flange plate fillet weld. Magnetic particles highlight two cracks.

served in Core 25 extended into the flange plate. The single weld crack detected in Core 23 terminated near the weld toe and did not extend into the flange plate.

Fractographic Examination

Cores 17 and 25, which contained the largest cracks, were opened to expose the crack surface. Figure 9 shows the crack surfaces from Core 17, where the transverse weld metal cracks and crack propagation into the flange are outlined clearly. The crack tip on one side was included; however, on the other side it can be seen to extend to the edge of the core. The crack surfaces show heavy accumulation of corrosion product, indicating exposure to the environment for several years. The crack surface is also very coarse in appearance, unlike most fatigue crack surfaces. The crack geometry shows that it propagated to within 10 mm (3/8 in.) of the underside surface of the bottom flange. No indication of crack propagation beyond the weld metal and into the web plate is indicated.

The crack surfaces from Core 25 were similar in appearance, as seen in Figure 10. The crack tip was inadvertently removed while obtaining a slice of the core for material testing. The crack tip extended into the flange about 3 mm (1/8 in.) farther than shown and to within 6 mm (1/4 in.) of the underside surface of the bottom flange plate. Heavy oxidation of the crack surface is also exhibited. Figure 10 shows two views of the fractured core; the crack in Core 25 extended into the girder flange similarly to the curved path exhibited in Core 17.

Because of heavy oxidation over most of the crack surface in both cores, fractographic examination was concentrated near the core edges and crack tips where corrosion was less severe. After as much of the corrosion product as possible was removed ultrasonically, the crack surfaces were examined with the scanning electron microscope (SEM). Figure 11 is a micrograph of the crack surface of Core 17 at the location marked "A" in Figure 9. Even though some corrosion product remains on the fracture surface, cleavage fracture is seen clearly in the micrographs. Evidence of cleavage fracture was noted at all other locations within the original crack. No evidence of stable crack extension (fatigue growth) was observed. Examination of the transverse weld metal crack surface did not yield information on the mechanism of fracture at this location because of excessive corrosion.

In an attempt to determine if any crack extension beyond the area of brittle fracture occurred under cyclic

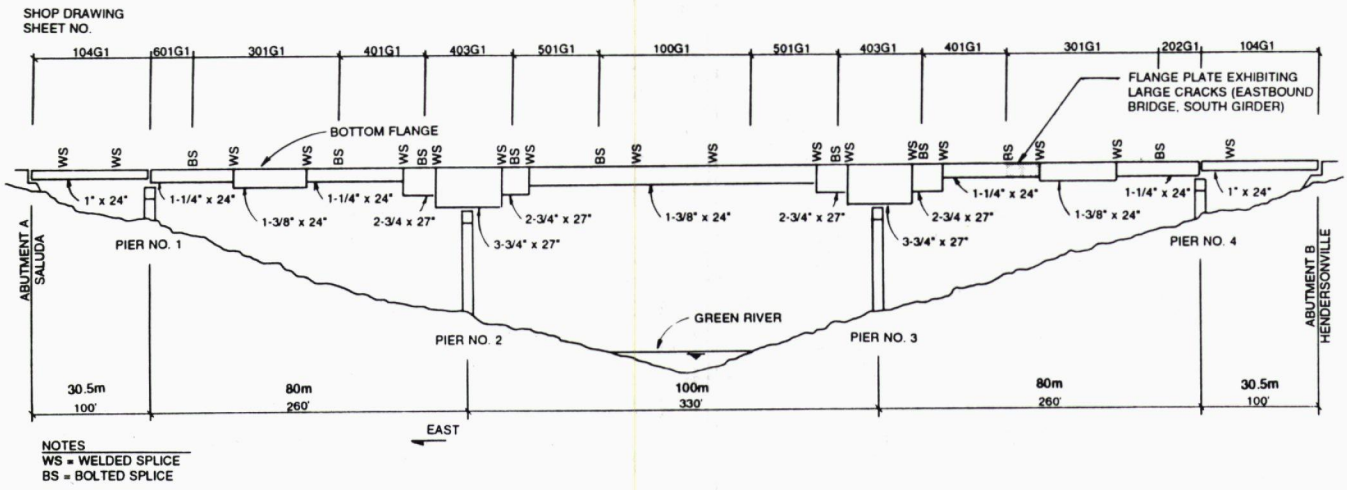

FIGURE 5 Partial evaluation of bridge showing bottom flange plate splices and dimensions.

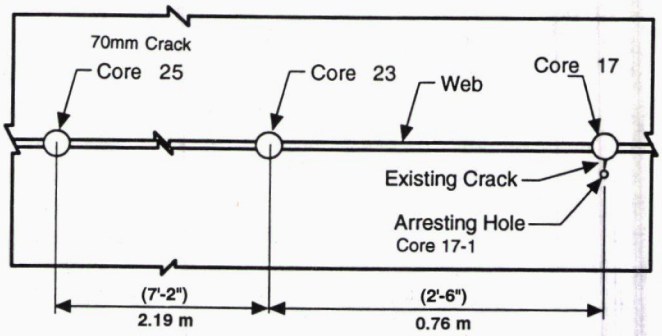

FIGURE 6 Partial schematic plan of Girder 301G1-3 at location where Cores 17, 17-1, 23, and 25 were removed.

FIGURE 7 Core 17 showing transverse weld metal crack extending into flange; Cores 23 and 25 are similar. Arrow on web indicates west direction.

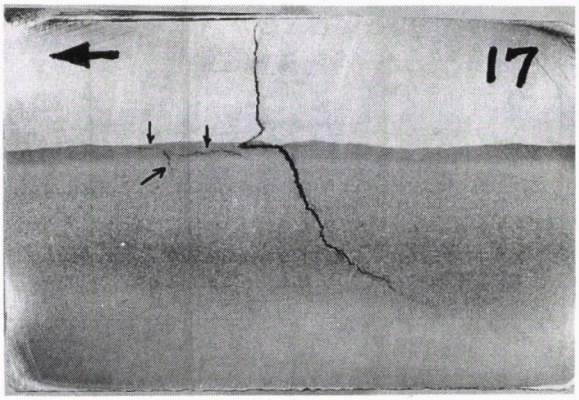

FIGURE 8 Longitudinal section through Core 17 showing transverse weld metal crack and propagation of crack into flange. Arrows show HAZ crack that propagated into base metal adjacent to primary crack.

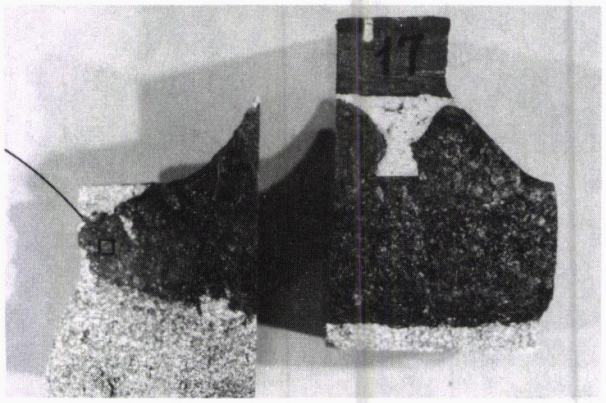

FIGURE 9 Exposed crack surface of Core 17 showing heavy oxidation.

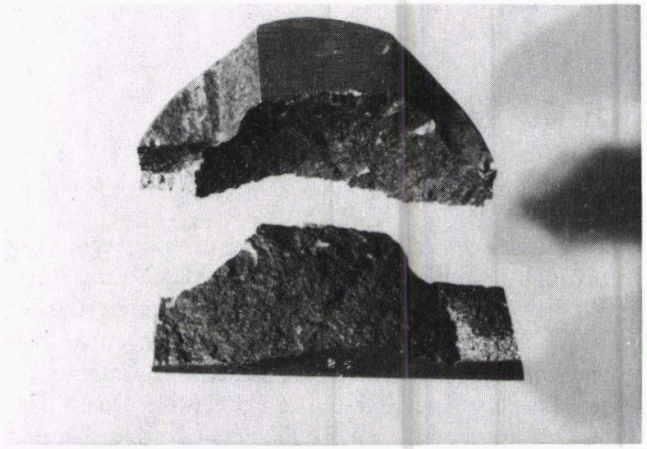

FIGURE 10 Exposed crack surface of Core 25 showing path of crack into flange plate.

loading, the boundary region of the original cracks was also examined. The crack surface within the small core (Core 17-1) removed at the crack tip of the large crack associated with Core 17 was examined. The micrograph of the crack surface again indicated cleavage fracture. The micrograph of the boundary between the crack surface and low-temperature fracture generated in separating the core crack surfaces did not indicate stable crack extension. Examination along the crack boundary of other core samples also did not reveal any clear evidence of fatigue crack extension. However, examination of Core 25 indicated possible evidence of fatigue crack growth at the boundary between the original crack and low-temperature fracture region. The heavy corrosion of the crack surface made it impossible to verify this elsewhere on the crack surface.

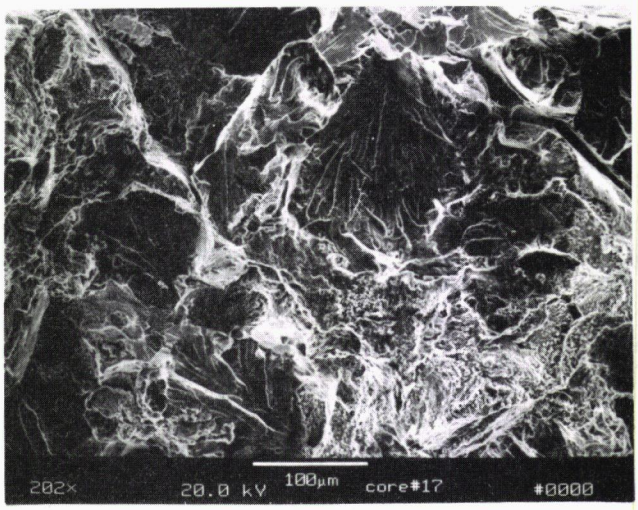

FIGURE 11 SEM micrograph of Area A (see Figure 9) of Core 17 showing cleavage fracture and corrosion product on crack surface (150×).

Material Testing

Charpy V-Notch Tests

Since the flange cracks in Cores 17 and 25 were close to through-thickness, Charpy V-notch (CVN) specimens could be machined only from Core 23 material. Six L-T orientation CVN specimens were made. Three specimens could be machined from the web plate of the girder. Specimens were tested at 4.5°C (40°F) (AASHTO Zone 2 test temperature). The average absorbed energy at 4.5°C for the flange plate specimens was 4 J (3 ft-lb), and the specimens exhibited a very coarse fracture surface appearance. At 54°C (130°F) the average absorbed energy was 10 J (8 ft-lb). Specimens machined from the 16-mm (5/8-in.) web plate indicated high toughness with an average of 67 J (50 ft-lb) at 4.5°C. The web plate material is well above the AASHTO Zone 2 requirement of 33 J (25 ft-lb) at 4.5°C for fracture-critical members.

Microstructure and Chemical Composition

The microstructure of the 32-mm (1 1/4-in.) flange plate obtained from Core 17 at mid-thickness is shown in Figure 12. The microstructure is predominantly pearlite with a small amount of ferrite outlining large prior austenite grain boundaries. The microstructure is typical of an annealed medium carbon steel (0.40 to 0.80 weight percent carbon) and explains the very low CVN test results obtained.

An analysis of the chemical composition of the flange material was also performed in addition to the web plate and flange to web weld metal from Core 17. The results of the analysis are given in Table 1.

The composition of the flange plate does not satisfy the requirements of ASTM A441 modified Corten B specified for the girders or any other structural-quality steel. However, the web plate meets the compositional requirements of this specification. The weld metal analysis shows a fairly high carbon content, most likely the result of pickup from the high-carbon flange material. The high carbon content of the flange plate and subsequent high carbon content of the weld metal is largely responsible for the transverse weld metal and heat-affected zone (HAZ) cracks observed in the core samples, as their susceptibility to hydrogen-induced cracking increases markedly with higher carbon content.

Hardness Testing

Rockwell hardness measurements were conducted on the flange plate for each core sample. An average hardness of Rockwell B, R_B 91 was measured. This hardness value is high and corresponds to a tensile strength of approximately 635 MPa (92 ksi).

Additional Core Samples

Five additional core samples were removed from the bottom flange of several girder sections in the eastbound bridge for material characterization to determine whether the improper flange material used in Girder

FIGURE 12 Flange plate microstructure of Core 17 (77×).

TABLE 1 Results of Analysis of Chemical Composition of Flange Material

Element	Flange Plate	Web Plate	Weld Metal	ASTM A441 Mod.
Carbon	0.47	0.20	0.19	0.10-0.19
Manganese	0.69	1.23	1.20	0.90-1.25
Phosphorus	0.012	0.016	0.013	0.04 max
Sulfur	0.023	0.047	0.026	0.05 max
Silicon	0.22	0.22	0.30	0.15-0.30
Nickel	0.03	0.04	0.79	--
Chromium	0.06	0.59	0.33	0.40-0.65
Molybdenum	0.01	0.03	0.17	--
Copper	0.04	0.30	0.26	0.25-0.40
Vanadium	<0.01	0.04	0.02	0.02-0.10
Aluminum	0.01	0.03	0.01	--
Niobium	0.005	0.008	0.009	--

301G1-3 was isolated to that girder or used in other girders in the bridge. Chemical composition, microstructure, hardness, and CVN tests were performed on the core samples.

Charpy V-Notch Tests

All five core samples showed an adequate level of toughness at 4.5°C (40°F). None of the additional cores tested provided results like those obtained from Core 23. The lowest toughness value was 20 J (15 ft-lb) at 4.5°C, which is well above the 4 J (3 ft-lb) at 4.5°C measured in Core 23.

Microstructure and Chemical Composition

Metallographic specimens were prepared for each additional core sample. The microstructures all consist of ferrite and pearlite in nearly the same proportions, with varying ferrite grain size in each plate thickness. This grain structure is the expected microstructure for the ASTM A441 Modified Corten B material specified.

An analysis of the chemical composition of the additional flange plate cores showed that the composition of the flange material is similar and within the A441 specification. The chemical compositions recorded should not have harmed the weldability if proper welding procedures were followed.

Hardness Measurements

The hardness measurements performed on these samples were less in all cases and more typical of A588-type material. Hardness values ranged from R_B 84.5 to 89.2 with an average value of 86.6 for these samples. The higher hardness of the 32-mm (1¼-in.) flange plate material provided a nondestructive means of detecting this type of material at other locations in the bridge using portable hardness-testing equipment. Field hardness measurements were performed on all 124 bottom flange plates. High hardness readings were measured, similar to those recorded in Core 17, in five plates. Field testing measurements of the flange plates where the cores were removed showed good correlation between the laboratory and field measurements.

Instrumentation and Field Testing

A testing program was carried out in December 1992 to measure live load stress ranges at selected bridge cross sections on the westbound structure. Strain measurements were recorded under dynamic loadings using heavily loaded control trucks and normal traffic. Layout of the strain gauges and numbering system is shown in Figure 13. Most instrumentation was placed on the north girder under the right, or truck, lane. In total, 16 strain gauges with 6-mm (¼-in.) gauge lengths were installed.

Two six-wheel dump trucks, similar to H-20 vehicles, were used as the control trucks. Each truck was loaded, providing a gross vehicle weight of approximately 227 KN (51 kips). Maximum responses using the control vehicles were obtained for a passage of the two trucks side by side. Gauge responses for the side-by-side control load are shown for instrumented Sections A and B in Figures 14 and 15, respectively.

Strain was recorded under normal traffic for a continuous period of 24 hr. Gauge measurements for a typical passage of heavy vehicle during this period are provided in Figures 14 and 15. In addition, the 24-hr data were scanned for the largest strain event during the test period. Four maximum responses were noted in this pe-

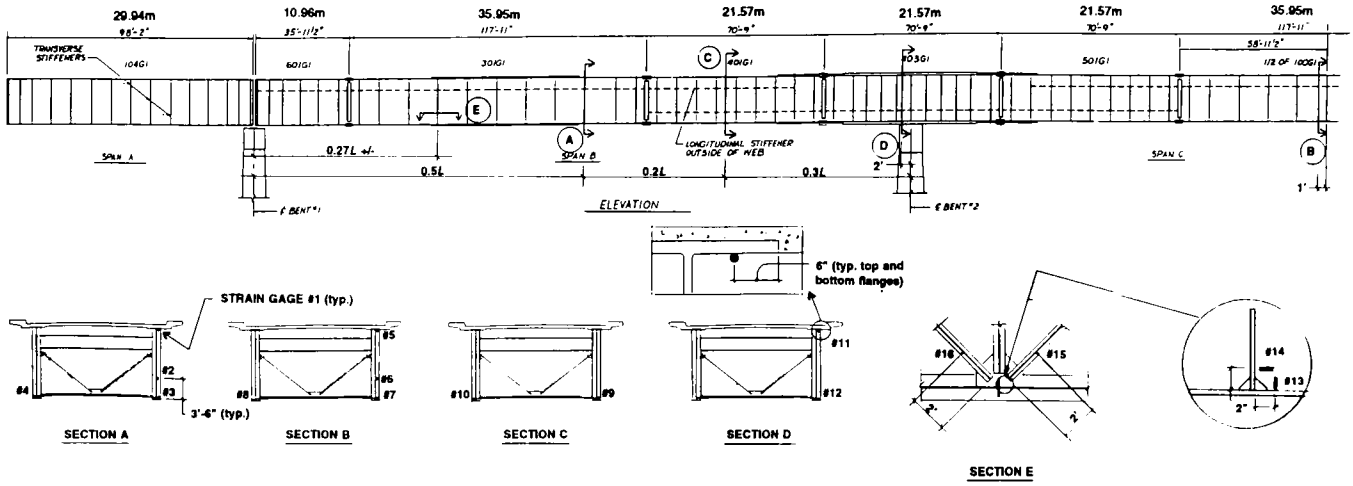

FIGURE 13 Strain gauge layout.

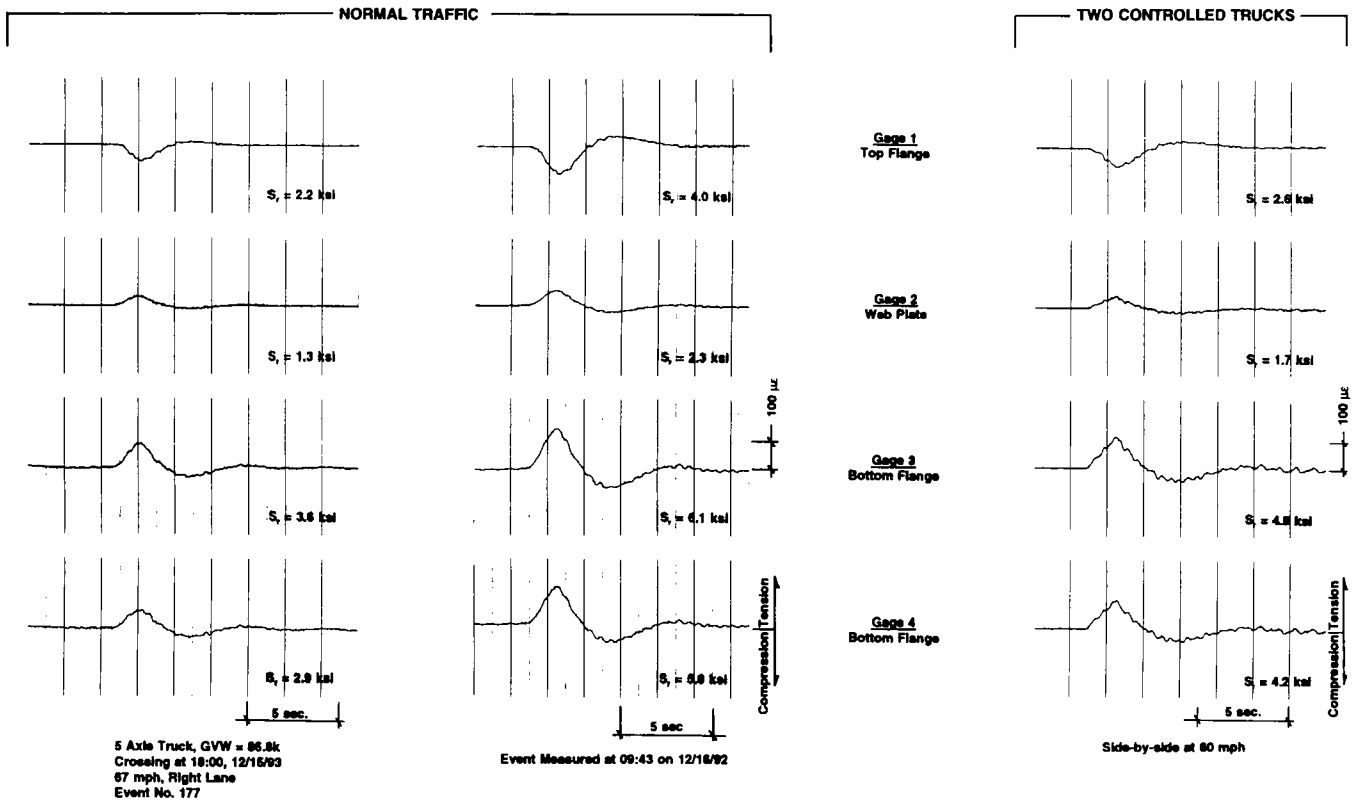

FIGURE 14 Dynamic strain gauge data measured at Section A (1 ksi = 6.9 MPa).

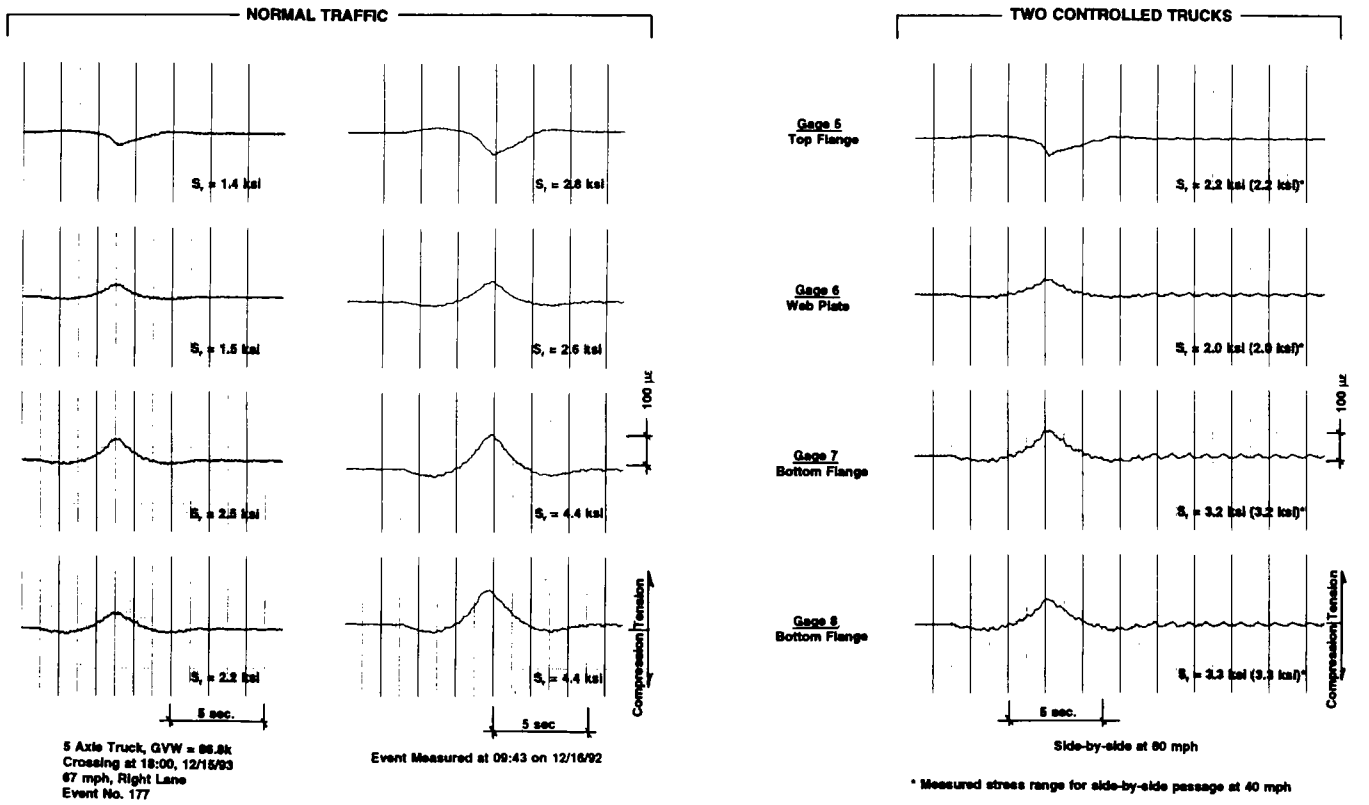

FIGURE 15 Dynamic strain gauge data measured at Section B (1 ksi = 6.9 MPa).

riod, and one record is shown in Figures 14 and 15 for the instrumented Sections A and B. These maximum responses most likely resulted from the passage of two heavy trucks crossing the bridge approximately side by side.

On the basis of the testing program carried out on the westbound bridge of the Green River structure, a summary of stress ranges for the 16 gauged locations is provided in Table 2. Gauge 3 at Section A located at midspan of the 80-m (260-ft) side span of the continuous unit measured the highest tensile stress ranges for all loadings:

- 18.7 MPa (2.7 ksi) under a control single truck loading,
- 33.1 MPa (4.8 ksi) under a control side-by-side loading,
- 25.5 MPa (3.7 ksi) for a single heavy truck from normal traffic, and
- 42.1 MPa (6.1 ksi) for a maximum event from normal traffic.

Maximum stress ranges for the 100-m (330-ft) main span measured for all loadings were recorded at Gauge 7 at Section B:

- 13.1 MPa (1.9 ksi) under a control single truck loading,
- 22.1 MPa (3.2 ksi) under a control side-by-side loading,
- 17.9 MPa (2.7 ksi) for a single heavy truck from normal traffic, and
- 30.4 MPa (4.4 ksi) for a maximum event from normal traffic.

Even though the structure was not designed composite, the structure shows some composite action between the girder and bridge deck. The continuous span unit indicates that the neutral axis occurs about 1.5 m (5 ft) below the top flange of the 4.3-m-deep girder.

Fracture Analysis

The large cracks observed in Girder 301G1-3 at Cores 17 and 25 were evaluated for fatigue and fracture susceptibility. Figure 3 shows a schematic of the cracks projected on a plane perpendicular to the bending stresses in the girder flange. As discussed previously, the crack tip nearest the bottom surface of the flange exhibits a nearly horizontal orientation and hence is not

TABLE 2 Summary of Measured Stress Ranges Under Controlled and Normal Heavy Truck Traffic Loadings

Measured Stress Range MPa (ksi)[1]								
	Controlled Loads				Normal Traffic Heavy Load[2]		Maximum Normal	
Strain Gage	Truck 1 R.L		Side-by-side		Single Vehicle		Traffic Loads[3]	
1	-8.3	(-1.2)	-17.9	(-2.6)	-13.8	(-2.0)	-27.6	(-4.0)
2	6.9	(1.0)	11.7	(1.7)	8.3	(1.2)	15.9	(2.3)
3	18.7	(2.7)	33.1	(4.8)	25.5	(3.7)	42.1	(6.1)
4	11.7	(1.7)	29.0	(4.2)	20.0	(2.9)	40.0	(5.8)
5	-6.2	(-0.9)	-15.2	(-2.2)	-10.4	(-1.5)	-19.3	(-2.8)
6	8.3	(1.2)	13.8	(2.0)	10.4	(1.5)	17.9	(2.6)
7	13.1	(1.9)	22.1	(3.2)	17.9	(2.6)	30.4	(4.4)
8	9.0	(1.3)	22.8	(3.3)	15.2	(2.2)	30.4	(4.4)
9	13.8	(2.0)	24.8	(3.6)	20.0	(2.9)	31.7	(4.6)
10	11.0	(1.6)	24.8	(3.6)	17.9	(2.6)	33.1	(4.8)
11	3.5	(0.5)	6.9	(1.0)	4.8	(0.7)	9.7	(1.4)
12	-4.1	(-0.6)	-10.4	(-1.5)	-6.9	(-1.0)	-13.1	(-1.9)
13	-2.8	(-0.4)	-5.5	(-0.8)	-3.5	(-0.5)	-6.2	(-0.9)
14	9.7	(1.4)	19.3	(2.8)	13.8	(2.0)	24.1	(3.5)
15	11.7	(1.7)	9.7	(1.4)	11.7	(1.7)	11.0	(1.6)
16	-9.7	(-1.4)	9.7	(1.4)	-11.0	(-1.6)	9.0	(1.3)

[1] Positive value denotes tension, negative value denotes compression
[2] Event No. taken from the NCDOT weigh-in-motion data.
[3] Maximum events scanned from the 24 hr data. These responses apparently resulted from the passage of two normal traffic trucks crossing the bridge approximately side-by-side.

particularly sensitive to crack extension as the stress intensity factor is much reduced.

Material fracture toughness in the flange plate is very low, 4 J (3 ft-lb) at 4.5°C (40°F). This brittle behavior is due to the coarse grain structure and chemical composition of the 32-mm (1¼-in.) flange plate of Girder 301G1-3. The toughness characteristics of this material appear very similar to the jumbo sections of A572 steel, as reported by Fisher and Pense (*1*).

From the dynamic and static fracture toughness estimates obtained for the jumbo sections, the CVN test results from Girder 301G1-3 are directly comparable to the test results from the jumbo sections. Since K_c test results are available from the jumbo sections, it is concluded that the static fracture toughness of the flange plate is about 44 MPa $\sqrt{m}$ (40 ksi $\sqrt{in.}$) (*1*).

The most severe crack appears to be in Core 25 (Figure 14), where a circumscribed elliptical-shaped crack is exhibited. At that location the crack tip is nearly perpendicular to the bending stresses in the girder flange and hence most likely to be susceptible to crack extension.

For an elliptical-shaped crack, the stress intensity factor is given by

$$K = F_e \sigma \sqrt{\pi a} \tag{1}$$

where a equals the minor semidiameter

$$F_e = \frac{[\sin^2 \theta + (a/c)^2 \cos^2 \theta]^{1/4}}{E(k)} \tag{2}$$

$$E(k) = \int_0^{\frac{\pi}{2}} (1 - k^2 \sin^2 \theta)\, d\theta, \; k^2 = \frac{c^2 - a^2}{c^2}$$

$$\cong \frac{3\pi}{8} + \frac{\pi}{8}\left(\frac{a}{c}\right)^2, \; c < 2a \tag{3}$$

This crack model is reasonable and verified by experimental studies on welded details since the web is restraining the crack opening.

For Core 25, a = 25.4 mm (1 in.) and c = 35.6 mm (1.4 in.). At Point A, where some evidence of crack extension may exist, Equation 2 results in F_e = 0.71.

Therefore, Equation 1 yields

$$K = 0.71\ \sigma\sqrt{\pi a} = 0.282\ \sigma = \text{MPa}\ (1.257\ \sigma = \text{ksi}) \quad (4)$$

On the basis of the dead load stress at these cracked locations in Girder 301G1-3 of about 93 MPa (13.5 ksi) and the maximum stress range measured at Section A, ignoring reversal, the maximum stress at Core 25 is about 128 MPa (18.5 ksi). Therefore, the maximum stress intensity is

$$K_{max} \sim 26.4\ \text{MPa}\ \sqrt{\text{m}}\ (24\ \text{ksi}\ \sqrt{\text{in.}})$$
$$< K_c \sim 44\ \text{MPa}\ \sqrt{\text{m}}\ (40\ \text{ksi}\ \sqrt{\text{in.}}) \quad (5)$$

The large crack in Core 17 with a smaller minor diameter and a larger major diameter provides a smaller estimate of stress intensity. Therefore, the fact that these cracks had been in the structure since it was constructed and did not result in a brittle fracture is reasonable.

No evidence of fatigue crack extension was observed in Cores 17 and 17-1 with the more favorable crack geometry. At Core 25, the stress intensity range is provided by

$$\Delta K = 0.282\ S_r = \text{MPa}\ (1.257\ S_r = \text{ksi}) \quad (6)$$

This provides a stress intensity range of 6.6 MPa $\sqrt{\text{m}}$ (6 ksi $\sqrt{\text{in.}}$) for the maximum stress range of 33 MPa (4.8 ksi) determined by the field testing. This does exceed the crack growth threshold ΔK_{th} = 3.3 MPa $\sqrt{\text{m}}$ (3 ksi $\sqrt{\text{in.}}$). Hence, it is very possible that some crack extension developed at the crack tip in Core 25 where the crack tip was perpendicular to the bending stress [under infrequent heavy loads analogous to the two control trucks side by side or the four maximum events 42 MPa (6.1 ksi) measured during the 24-hr period]. Fortunately, these events apparently do not occur often enough to result in major crack extension. No crack extension was detected where the crack tip was nearly horizontal. Brittle fracture was avoided because of the near horizontal orientation of the cracks adjacent to the bottom surface of the tension flange where ΔK would be much smaller.

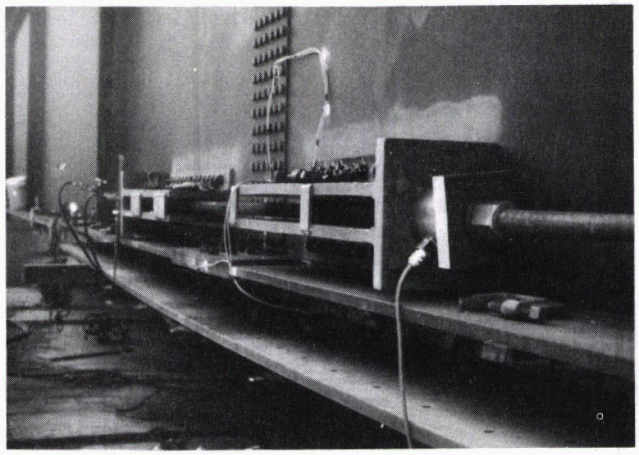

FIGURE 16 Post-tensioning assembly installed at girder bolted splice connection used to install coverplate retrofit.

Summary of Findings

The test results from the examination of core samples containing cracks and additional cores to evaluate material properties as well as the field testing measurements of stress range, the hardness survey, and nondestructive evaluation have demonstrated that the cracks discovered in the I-26 Green River Bridge occurred at the time of fabrication. Specific findings are as follows:

- Fractographic examination indicates that the two large cracks removed from Girder 301G1-3 developed at the time of fabrication. These large cracks resulted from the use of a steel plate material containing very high carbon levels, large grain structure, and very low toughness. This material did not meet ASTM A441 modified Corten B steel requirements, and it was not a weldable steel.
- All of the evaluated cracks appear to have resulted from hydrogen-related cold cracking. The many transverse cracks in longitudinal fillet welds of all the bridge girders appear to be cold cracks.
- The large cracks in Girder 301G1-3 were tolerant of dead and live load stresses, mainly because the crack tip had a favorable orientation to applied forces. This orientation prevented fatigue crack growth and brittle fracture.
- All tested web plate material revealed good toughness that exceeded the CVN requirements for Zone 2. The web toughness was beneficial and prevented more serious crack extension in the girders.
- The additional core samples removed randomly from other flange plates with thicknesses between 32 and 95 mm (1¼ and 3¾ in.) all exhibited acceptable levels of notch toughness.

Recommendations for Retrofitting

The fatigue life of the Green River Bridge can be extended greatly by retrofitting the fracture-critical primary girders. A two-girder nonredundant system containing numerous small cracks requires retrofit measures that will provide redundancy in all spans and will reduce the stress ranges, further reducing the pos-

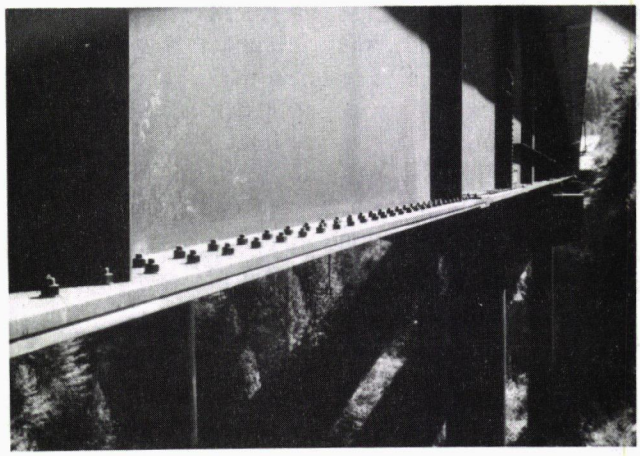

FIGURE 17 Completed bottom flange coverplate installation.

sibility of fatigue crack extension from the flange–to–web plate fillet weld cracks.

The numerous flange–to–web plate fillet weld cracks cannot be removed by coring or drilling. Therefore, all bottom flanges subjected to tensile stresses should be coverplated using full-flange-width coverplates connected with high-strength bolts. The top tension flanges of the girders over the piers do not require any modification, as no cracks were detected in any of these flanges. This retrofit measure provides an alternative load path in all tension regions of the main girder.

The recommended retrofitting was included in the construction work to rehabilitate the bridge. The project consisted primarily of cover plating the main girders and concrete bridge deck repairs. The cover plates match the typical flange width of 610 mm (24 in.) and range in thickness from 25 to 38 mm (1 to 1½ in.). Four rows of bolts are used to attach the plates. These rows are positioned 100 and 200 mm (4 and 8 in.) from each flange edge using a typical bolt spacing of 300 mm (12 in.) on center along each row. Alternate bolt rows are staggered by 150 mm (6 in.) longitudinally. The total weight of coverplates for both bridges (four girder lines) is 1605 KN (360,500 lb) of structural steel, and the attachment used 16,200 ASTM A325 bolts of 22-mm (⅞-in.) diameter.

All coverplate material was specified to meet ASTM A588 and CVN requirements of 33 J (25 ft-lb) at 4.5°C (40°F). In addition, all coverplate material and fabrication was required to meet AASHTO requirements (2).

NCDOT developed the coverplate retrofit details and installation procedure. The coverplate retrofit was designed to run continuous through girder bolted splice connection regions with the new coverplate positioned tight against the bottom flange. This was accomplished by post-tensioning the splice area, removing the bottom flange connection plate, clamping the coverplate into position, and match drilling the existing connection bolt pattern, and reinstalling the existing bottom flange connection plates. Figure 16 shows the post-tensioning bracket assembly installed at a bolted splice connection just prior to a bottom flange connection plate removal. Note that the new coverplate is positioned about 8 in. below the girder bottom flange, ready for final positioning.

All coverplate drilling was performed dry without coolant or lubricant for the hole cutters. A completed girder bottom flange retrofit is shown in Figure 17. The construction cost to fabricate the material and install the coverplates was $600,000. All superstructure retrofitting and bridge deck rehabilitation work was completed in October 1994 and paid for by NCDOT.

ACKNOWLEDGMENTS

NCDOT was responsible for designing the retrofit scheme. Lehigh University carried out the materials tests and metallographic and fractographic assessments. Wiss, Janney, Elstner Associates (WJE) carried out the instrumentation and field testing, removed the cores, and made the field hardness surveys.

The authors wish to recognize and extend their appreciation to all of the people who assisted with and contributed to this evaluation. Personnel of NCDOT, including Gary Rudisill, Neb Bullock, Mark Robbins, and Rodger Rochelle, were very helpful. WJE staff that contributed substantially to the project were Richard Walther, Roger Pelletier, and Robert Gessel. B. T. Yen assisted with the Lehigh University work.

REFERENCES

1. Fisher, J. W., and A. W. Pense. Experience with the Use of Heavy W Shapes in Tension. *Engineering Journal*, American Institute of Steel Construction, Vol. 24, No. 2, 1987.
2. *Guide Specifications for Fracture Critical Nonredundant Steel Bridge Members*. AASHTO, Washington, D.C., 1986.